JOURNAL OF CATALYSIS 96, 122–138 (1985)

Temperature-Programmed Sulfiding and Reduction of CoO/Al_2O_3 Catalysts

P. ARNOLDY, J. L. DE BOOYS, B. SCHEFFER, AND J. A. MOULIJN

Institute for Chemical Technology, University of Amsterdam, Nieuwe Achtergracht 166, 1018 WV Amsterdam, The Netherlands

Received January 2, 1985; revised April 22, 1985

Sulfiding of CoO/Al_2O_3 catalysts has been studied by means of Temperature-Programmed Sulfiding (TPS). TPS patterns were compared with Temperature-Programmed Reduction (TPR) patterns, which give information on the presence of several oxidic Co phases. Sulfiding takes place in a low-temperature region (LT; 295–750 K) and in a high-temperature region (HT; 750–1200 K). Most surface species as well as supported crystallites sulfide in the LT region, whereas in the HT region there is sulfiding of Co^{2+} ions in subsurface positions and of, probably tetrahedrally coordinated, Co^{2+} surface ions. For low calcination temperatures (below 800 K) sulfiding in the LT region predominates. The sulfiding pattern shifts from the LT to the HT region with increasing calcination temperature (800–1000 K) due to solid-state diffusion of Co^{2+} ions. The influence of Co content on the sulfiding rate is relatively small. The sulfiding rate increases slightly with H_2O content, which is tentatively explained by polarization of H_2S by H_2O in the adsorbed state. Generally, sulfiding in H_2S/H_2 (measured by TPS) is much faster than reduction in H_2 (measured by TPR) because of different reaction mechanisms. In sulfiding, H_2S is the primary reactant in O–S exchange reactions, whereas H_2 plays only a secondary role, e.g., in reduction of elemental sulfur. H_2 can only compete with H_2S as primary reactant when H_2S diffusion is hindered, i.e., in the case of large crystallites. At 1000–1270 K, interconversion of various Co sulfides can be observed. These processes are different for catalysts and bulk compounds, pointing to strong interaction of Co ions with the support.

INTRODUCTION

The hydrodesulfurization (HDS) activity of $CoO–MoO_3/Al_2O_3$ catalysts is much higher than that of the model systems MoO_3/Al_2O_3 and CoO/Al_2O_3 (*1, 2*). However, particularly the structures of the Co-containing species in CoO/Al_2O_3 and $CoO–MoO_3/Al_2O_3$ are not well characterized as yet. It has been suggested that a sulfidable, nonreducible oxidic Co species is the precursor of a sulfided Co species referred to as Co–Mo–S or Co_S, which is the most HDS-active species present (*2–6*). It has recently been shown, on the basis of Temperature-Programmed Reduction (TPR) measurements, that the structure of oxidic CoO/Al_2O_3 catalysts is unexpectedly complicated (*7*); at least four oxidic Co phases could be distinguished which differ widely in their reducibility and which could be divided into eight subphases (see also Table 2 of the present article).

The aim of the present study is to investigate sulfiding of various CoO/Al_2O_3 catalysts by means of Temperature-Programmed Sulfiding (TPS). This technique has been successful in the study of sulfiding of MoO_3/Al_2O_3 catalysts (*8*). TPS results on CoO/Al_2O_3 and MoO_3/Al_2O_3 form the basis for the interpretation of the TPS results on $CoO–MoO_3/Al_2O_3$, which have been published elsewhere (*9*). The TPS results on CoO/Al_2O_3 will be compared with TPR measurements. This will give insight into the relative sulfiding rates of the various oxidic Co species (distinguished by TPR) and on the role of H_2 in sulfiding.

EXPERIMENTAL

a. Materials

Co_3O_4, $Co(NO_3)_2 \cdot 6H_2O$, and α-S were

0021-9517/85 $3.00

TABLE 1

Quantitative TPS Results

Materials		Pretreatment temp.[a] (K)	TPR (Figs.)	TPS (Figs.)	H_2S uptake (mol H_2S/mol Co)[b,c]				
					A	B	C	D	E
Reference compounds									
CoO		1270	Ref. (7)	3a	0.00	0.00	0.81	0.81	0.12
Co_3O_4		295	Ref. (7)	3b	0.00	0.00	0.64	0.64	0.12
$CoAl_2O_4$		295	Ref. (7)	3c	0.00	0.00	0.73	0.73	0.15
γ-Al_2O_3		295	Ref. (7)	Ref. (8)	40[b]	−40[b]	0	0	0
γ-Al_2O_3		775	Ref. (7)	Ref. (8)	370[b]	−370[b]	0	0	0
CoO/Al_2O_3 catalyst									
at./nm^2	wt% CoO								
0.20	0.50	725	2a	7a	7.57	n.d.	n.d.	n.d.	0.04
0.62	1.47	675	2b	6a,7b	0.82	−0.16	0.19	0.85	0.04
1.24	2.92	295	2c	—	0.43	−0.13	n.d.	n.d.	0.09
1.24	2.92	725	2c	6b,7c	1.47	−1.09	0.36	0.74	0.08
2.52	5.75	725	2d	6c,7d	0.75	−0.35	0.40	0.80	0.09
3.84	8.53	295	1a,2e	4a,5b	0.17	−0.04	0.58	0.71	0.10
3.84	8.53	675	1a,2e	5c,6d,7e	0.40	−0.21	0.47	0.66	0.11
3.84	8.53	825	1b	5d	0.43	−0.30	0.58	0.71	0.12
3.84	8.53	925	1c	4b,5e	0.46	−0.29	0.74	0.91	0.12
3.84	8.53	1025	1d	5f	0.35	−0.33	0.77	0.79	0.12
3.84	8.53	1175	1e	5g	0.28	−0.25	0.83	0.86	0.11

[a] *In situ* pretreatment, preceded by *ex situ* calcination at 725 K in the case of CoO/Al_2O_3 catalysts.
[b] The H_2S uptake figures for γ-Al_2O_3 are given in μmol H_2S/g Al_2O_3; n.d. = not determined.
[c] A = Uptake at 295 K, except for the Co(0.62)/Al sample (uptake at 675 K). B = Desorption after the isothermal uptake (A), calculated from H_2S pressures which lie below the H_2S influent level. C = Uptake between the end temperature of desorption (B) and 1270 K, corrected for H_2S production due to reduction of γ-Al_2O_3 impurities (25 μmol/g Al_2O_3). D = A + B + C, i.e., the total uptake up to 1270 K due to sulfiding of Co species. E = Uptake during cooling after TPS, corrected for H_2S adsorption on γ-Al_2O_3 (30 μmol/g Al_2O_3). Compare with a value of 0.14 mol H_2S/mol Co related to the conversion of Co_4S_3 to Co_9S_8.

pro analysi chemicals. The preparation of CoO and $CoAl_2O_4$ has been described elsewhere (*7*). These compounds were XRD-pure, except the CoO sample which contained a small fraction of Co_3O_4. The Al_2O_3 support was a high-purity γ-Al_2O_3 (Ketjen 000-1.5E (CK 300); specific surface area 195 m^2/g; pore volume 0.50 cm^3/g; particle size 100–150 μm). CoO/Al_2O_3 catalysts were prepared by pore volume impregnation of γ-Al_2O_3 with a solution of $Co(NO_3)_2 \cdot 6H_2O$ in demineralized H_2O, followed by drying and calcining. The impregnation was executed stepwise (*5, 10, 11*), i.e., in this study Co contents above 1.5% CoO were reached by repetition of the impregnation–drying–calcination sequence (addition of ca. 1.5 g CoO per 100 g support in each sequence). The samples were denoted as Co(x)/Al, in which x indicates the Co content expressed in Co atoms/nm^2 (see Table 1).

Drying was performed in air at atmospheric pressure, by gradually increasing

the temperature from 325 to 380 K over a period of 3 h, followed by an isothermal period of 16 h at 380 K. Dried samples of 6–18 g were calcined in a quartz tube (internal diameter 10 mm) in a purified air flow (300 μmol/s). The temperature was increased at a heating rate of ca. 20 K/min up to the final temperature (725 K), which was maintained for 2 h. The Co(3.84)/Al sample was recalcined at various temperatures (675–1175 K) in purified Ar or N_2, followed by *in situ* TPR or TPS analysis.

b. X-Ray Diffraction (XRD)

XRD has been carried out in a Philips diffractometer PW 1050/25 using Co$K\alpha$ radiation. A Fe filter was applied to remove Co$K\beta$ radiation. Crystallite sizes have been calculated using the Scherrer equation with correction for natural line broadening and assuming that the crystallite shape factor K equals 1 (*12*).

c. Temperature-Programmed Reduction (TPR)

The TPR equipment has been described in detail elsewhere (*7*). As reducing gas a 67% H_2/Ar high-purity mixture was used (flow rate 12 μmol/s; pressure 1.0 bar). The samples generally contained 70 μmol Co; only in the case of Co(0.20)/Al 18 μmol was used. The temperature was increased at a rate of 10 K/min up to a final temperature of 1240 K, which was maintained until the reduction was finished. H_2O, CO_2, and organics (except CH_4), which evolved during reduction, were trapped in 3A and 5A molecular sieve columns. H_2 consumption as well as CH_4, CO, and O_2 production was measured as a positive peak by means of a thermal conductivity detector (TCD). A flame ionization detector (FID) was used for CH_4 detection only. CH_4 was retarded by the 5A molecular sieve (ca. 7 min). The FID pattern was corrected for this retardation, whereas the TCD signal, containing some CH_4 production besides mainly H_2 consumption, was not.

d. Temperature-Programmed Sulfiding (TPS)

The TPS equipment has been described in detail elsewhere (*8*). Sulfiding was started at room temperature (295 K) until H_2S uptake was finished. Then the temperature was increased at a rate of 10 K/min up to a final temperature of 1270 K, which was maintained for 30 min. Subsequently, the power supply to the furnace was switched off, resulting in cooling at a rate decreasing from 30 to 10 K/min in the temperature range 1270–800 K. The sulfiding mixture contained 3.4% H_2S, 28.7% H_2, and 67.9% Ar (flow rate 12 μmol/s; pressure 1.1 bar). H_2S and H_2O were detected in the effluent gas by a mass spectrometer. H_2 was measured with a thermal conductivity detector, after H_2S and H_2O had been trapped in a 5A molecular sieve column. The samples contained 100–350 μmol Co, in order to reach integral conversion of H_2S and to avoid total H_2S consumption. Integral H_2S conversion is necessary for sufficient accuracy of the mass spectrometer measurements. Quantitative TPS results have been obtained with an accuracy of ca. 15% in general, due to the mass spectrometer instability and the often broad signals involved, while for sharper peaks (see, e.g., Fig. 7) the accuracy was ca. 5%.

After calcination at 725 K, all samples had been exposed to the atmosphere and therefore were wet, i.e., they contain large amounts of adsorbed H_2O. Before sulfiding all samples were pretreated *in situ*: —flushing in Ar or N_2 at 295 K for 30 min ("wet" catalysts), or—flushing in Ar or N_2 at 675–1175 K for 2 h, followed by cooling to 295 K ("dry" catalysts, calcined at 725–1175 K).

RESULTS

a. X-Ray Diffraction

XRD of the crystalline reference compounds showed no line broadening, except the Co_3O_4 sample (calculated crystallite size 40 nm). XRD of the oxidic CoO/Al_2O_3

TABLE 2

Correlation of TPR and TPS Data on CoO/Al_2O_3 Catalysts

Co phase[a]	Description[a]	TPR reduction maximum (K)	TPS region[c]	TPS sulfiding maximum (K)
I	Co_3O_4 (c)	600	LT	500
IIA	surface Co^{3+}	750	LT	—
IIB	Co^{3+}–Al^{3+}-oxide (c)[d]	750	LT	700
III	surface Co^{2+}[e]	900	LT	—
IVA	surface Co^{2+}[e]	1130–1240	LT,HT	—
IVB	subsurface Co^{2+}	1130–1240	HT	1000
IVC	$Co_xAl_{(\frac{8}{3}-\frac{x}{3})}O_4$ (c)[f]	1230	HT	1060
IVD	$CoAl_2O_4$ (c)	1150	HT	1060

[a] Assignment of Co phases on the basis of extensive TPR work on CoO/Al_2O_3 (*7*). (c) = crystalline phase.

[b] From Ref. (*7*) and Figs. 1 and 2 of the present study.

[c] LT = Low-temperature sulfiding region (295–750 K). HT = High-temperature sulfiding region (750–1200 K).

[d] Proposed stoichiometry: Co_3AlO_6 (*7*).

[e] Phase IVA differs from phase III in the amount of Al^{3+} ions in the Co^{2+} surrounding (ca. 10 and ca. 7 Al^{3+}, respectively) (*7*).

[f] x is a small fraction of 1, e.g., $x = 0.18$ for Co(4.12)/Al (*7*).

samples calcined at 725 K indicated the presence of Co_3O_4 crystallites for Co contents of 2.52 and 3.84 at./nm^2. The influence of calcination temperature on XRD of CoO/Al_2O_3 has been reported elsewhere (*7*).

XRD has also been performed on samples which had been subjected to TPS analysis. After TPS, the sulfiding gas was replaced by Ar when the temperature was decreased to 675 K. Cooling was continued in Ar until room temperature was reached, after which the samples could be exposed to air without occurrence of bulk oxidation of crystalline sulfides to sulfates, such as $CoSO_4 \cdot H_2O$ and $CoSO_4 \cdot 6H_2O$.

After TPS of CoO, Co_3O_4, and $CoAl_2O_4$ and all CoO/Al_2O_3 catalysts, Co_9S_8 (*13*) was found. The Co_9S_8 bands were broadened in the case of sulfided CoO/Al_2O_3 (calculated crystallite size 20–40 nm). Their intensity increases as a function of Co content, from almost zero for Co(0.20)/Al to the intensity of the always present, broad δ-Al_2O_3 bands for Co(2.52–3.84)/Al. No γ- and α-Al_2O_3 nor Co–Al oxides of spinel type were found after sulfiding.

b. Temperature-Programmed Reduction

TPR patterns are given in Figs. 1 and 2. Co reduction is found over a broad temperature range; several reduction regions can be distinguished, as was reported for batchwise prepared Co(4.12)/Al catalysts (*7*). The regions I, II, III, and IV are found around 600, 750, 900, and 1200 K, and correspond with reduction of the Co phases I, II, III, and IV, respectively (see Table 2). Quantitative TPR analysis shows that, taking into account H_2 consumption and CH_4 production in cracking/reduction of organic impurities (*7*), the H_2 consumption related to Co reduction is ca. 1.0 mol H_2/mol Co when reduction in region IV predominates, whereas it increases to 1.1–1.2 mol H_2/mol Co when the contribution of the regions I and II increases.

Figure 1 gives TPR patterns of Co(3.84)/Al as a function of calcination temperature. In this series, calcination and TPR were carried out *in situ* which prevents adsorption of impurities (organics and H_2O) on the freshly calcined samples. Consequently, no

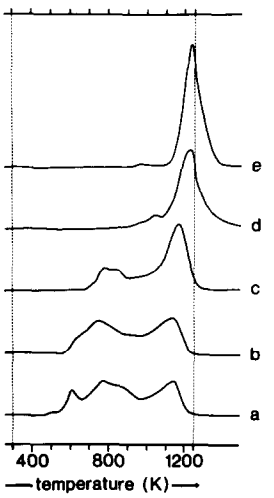

FIG. 1. TPR patterns (10 K/min) of Co(3.84)/Al catalysts as a function of calcination temperature. (a) 725 K; (b) 825 K; (c) 925 K; (d) 1025 K; (e) 1175 K. Only the TCD patterns are given. Between calcination and TPR measurements there has been no contact with the atmosphere.

FID signal due to CH_4 formation caused by cracking/reduction of organic impurities was found. As in the case of batchwise prepared Co(4.12)/Al (*7*), reduction of the stepwise-prepared Co(3.84)/Al occurs in all four TPR regions after calcination below 900 K, whereas only reduction in region IV remains after calcination above 1000 K. The stepwise-prepared catalyst contains more of the dispersed Co^{2+} phases (IVA/B) and less of the crystalline Co^{3+} phases (I/IIB) after calcination at 725–925 K, in comparison with the mentioned batchwise-prepared catalyst, so stepwise impregnation leads to a higher dispersion (*10*).

Figure 2 gives TPR patterns of Co/Al catalysts as a function of Co content (calcination temperature 725 K). This series was exposed to the laboratory atmosphere, resulting in adsorption of impurities (organics and H_2O) and, consequently, the observation of CH_4 production in TPR. Besides Co reduction, a small peak just above room temperature (due to O_2 desorption) and a significant peak around 1040–1100 K (due to reduction of impurities in the Al_2O_3 support) have been observed for the catalysts with lower Co content. The latter peak shifts to lower temperatures with increasing Co content, suggesting catalysis of this reduction by Co metal (*14*). In TPR of Co(0.20)/Al, the TCD and FID signal in the temperature range 650–1000 K is completely due to cracking of organics, whereas in TPR of Co(0.62–3.84)/Al reduction of these organics occurs with CH_4 as main product, because of formation of Co metal at low temperatures which acts as a catalyst for reduction of organics. For the Co(0.20)/Al sample, all Co reduction takes place in region IV around 1240 K, due to presence of phase IVA. With increasing Co content, the region IV peak shifts from 1240 to 1130 K and the fraction of Co present as phase IVA decreases from 100 to ca. 40%. The peaks from regions I, II, and III come up simultaneously for the higher Co contents. Comparison of TPR for a dry and a

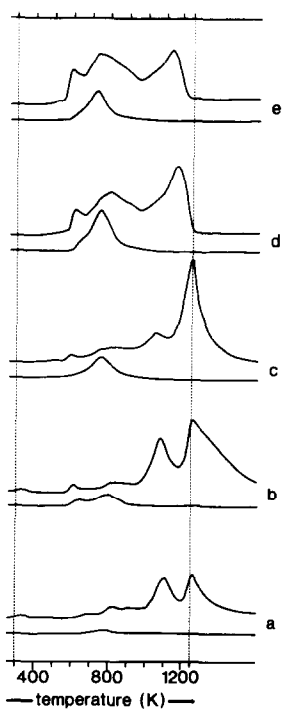

FIG. 2. TPR patterns (10 K/min) of Co/Al catalysts calcined at 725 K, as a function of Co content. (a) 0.20 at./nm^2; (b) 0.62 at./nm^2; (c) 1.24 at./nm^2; (d) 2.52 at./nm^2; (e) 3.84 at./nm^2. The upper and lower signal represent the TCD and FID signals, respectively.

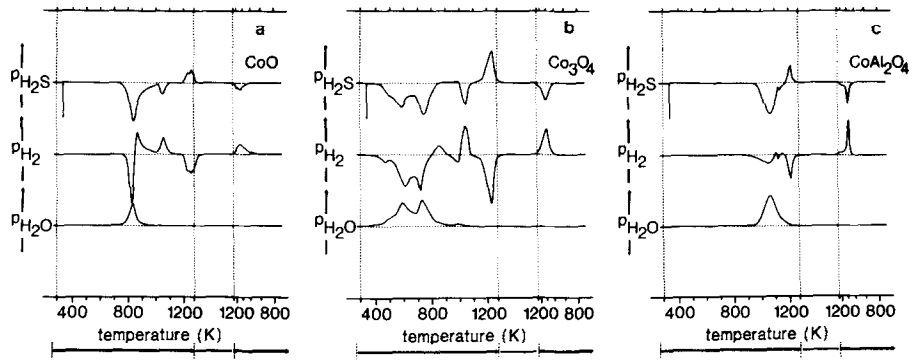

FIG. 3. TPS patterns (10 K/min; H_2S, H_2, and H_2O patterns) of crystalline reference materials. (a) CoO; (b) Co_3O_4; (c) $CoAl_2O_4$. The 50% conversion level of H_2S is indicated by a two-sided arrow.

wet catalyst (Figs. 1a and 2e, respectively) indicates that the H_2O content does not affect the reducibility significantly.

c. Temperature-Programmed Sulfiding

The TPS results are shown in Figs. 3–8, while some quantitative data are presented in Table 1. Color changes have been observed during sulfiding of light-colored samples at 295 K: Co(0.20–1.24)/Al samples calcined at 725 K turned from blue/green into grey/black. On the other hand, the bright blue color of $CoAl_2O_4$ and Co(3.84)/Al samples calcined at 1025–1175 K is not affected by sulfiding at 295 K.

Figure 3 gives the TPS patterns of the crystalline compounds CoO, Co_3O_4, and $CoAl_2O_4$. The general picture arising for sulfiding of these oxides is that H_2S consumption is accompanied by almost simultaneous H_2 consumption and H_2O production. Around 850–870 K, in TPS of CoO and Co_3O_4, H_2 production instead of consumption is found. The overall H_2 uptake due to sulfiding is much larger in the case of Co_3O_4 than in the case of CoO and $CoAl_2O_4$, due to the sulfiding of Co^{3+} ions in the former sample. Besides sulfiding of the oxides, interconversion of Co sulfide species is observed at 1000–1270 K, in the temperature program as well as during cooling. In these interconversions H_2S consumption (around 1050 K in the temperature program and during cooling) and H_2S production (around 1230 K in the temperature program) are always accompanied by H_2 production and consumption, respectively. Only in TPS of $CoAl_2O_4$ the first interconversion band (around 1050 K) is obscured or even missing, due to the occurrence of sulfiding itself around 1050 K. The TPS peak areas agree with the following interconversions: 1. $Co_9S_8 \rightarrow CoS_{1+x}$ (temperature program, >1000 K, maximum around 1050 K); 2. $CoS_{1+x} \rightarrow Co_4S_{3\pm x}$ (temperature program, >1150 K, maximum around 1230 K); 3. $Co_4S_{3\pm x} \rightarrow Co_9S_8$ (cooling pattern, >1000 K, maximum around 1100 K). In agreement herewith, the total H_2S uptake in the temperature program corresponds with formation of $Co_4S_{3\pm x}$ (see Table 1). The phases Co_9S_8, CoS_{1+x}, and $Co_4S_{3\pm x}$ are thermodynamically favored phases in the temperature range studied (*13, 15*). Because x is a small fraction of 1, the latter two phases will be denoted as CoS and Co_4S_3 in the following. The order of stability of these three phases with increasing temperature agrees with the literature (*15*); only the temperatures at which the interconversions have been reported to be allowed on thermodynamic grounds (1015 and 1190 K at a p_{H_2S}/p_{H_2} ratio of 0.12) are slightly higher than the start temperatures for these interconversions observed in the present study (1000 and 1150 K, respectively). For the conversion of Co_4S_3 to a so-called liquid phase (*13, 15*), reported

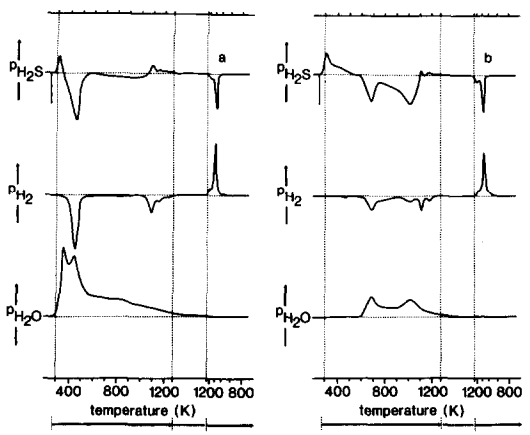

FIG. 4. TPS patterns (10 K/min; H_2S, H_2, and H_2O patterns) of Co(3.84)/Al catalysts. (a) Calcined at 725 K, wet; (b) calcined at 925 K, dry. The 50% conversion level of H_2S is indicated by a two-sided arrow.

to be stable above 1205 K (*15*), no evidence can be found in the present study, since the sulfur contents of Co_4S_3 (29 ± 1.5 wt% S at 1125 K) and of the liquid phase (29 ± 3 wt% S at 1270 K) are nearly equal.

The sulfiding reactivity decreases in the order Co_3O_4–CoO–$CoAl_2O_4$. A special feature of the TPS pattern of Co_3O_4 is the broad two-peak sulfiding band. However, it must be noted that the position of the sulfiding peak maxima and the TPS pattern shape can vary for different preparation procedures, especially in the case of CoO and Co_3O_4 samples. For instance, a CoO sample prepared from $Co(NO_3)_2 \cdot 6H_2O$ by heating in Ar at 1175 K for 2 h resulted in a TPS peak around 700 K (instead of the peak at 830 K, observed in Fig. 3a, for CoO prepared from Co_3O_4 by heating in N_2 at 1290 K for 2 h).

Figure 4 gives two typical examples of TPS patterns of Co(3.84)/Al samples differing in H_2O content and calcination temperature. Some H_2S uptake is found already during isothermal sulfiding at 295 K (not shown; see Table 1). At the start of the temperature program, H_2S and H_2O desorption peaks are present. Sulfiding takes place over a broad temperature range (295–1200 K). H_2S and H_2 consumption as well a H_2O production occur simultaneously. Around 450 and 680 K (see Figs. 4a and b, respectively), a distinct sulfiding peak is observed, in which the H_2 consumption is relatively large due to the sulfiding of Co^{3+} ions. H_2O is not only product of sulfiding, but also of dehydration of the support over the whole temperature range studied. At 1050–1270 K, H_2S production is related to H_2 consumption, obviously caused by interconversion of Co sulfide species. This pattern, however, is clearly different from the one found for the crystalline oxides (see Fig. 3). It can be deconvoluted into two peaks (around 1100 and 1170 K) superimposed on a broad H_2S production "background" which continues up to 1270 K. Upon cooling, H_2S consumption and H_2 production are found because of oxidation of Co sulfide species. The total H_2S consumption up to 1270 K corresponds approximately with the formation of Co_4S_3 in the case of Co/Al catalysts (see Table 1). The H_2S production and H_2 consumption in the temperature range 1050–1270 K did not exceed a value of ca. 0.12 mol H_2S or mol H_2 per mol Co.

In the following Figs. 5–7 only H_2S patterns will be given for the sake of simplicity. The corresponding H_2 and H_2O patterns are correlated with the H_2S patterns as in Figs. 4a–b.

Figure 5 gives TPS patterns of Co(3.84)/Al as a function of calcination temperature and pretreatment. The addition of elemental sulfur (see Fig. 5a) leads to the appearance of a sharp H_2S production and (not shown) H_2 consumption peak at 530 K, with respect to the normal TPS pattern of a wet catalyst (see Fig. 5b). Predrying (see Fig. 5c) results in sharpening and a shift to higher temperature of the sulfiding peak around 450 K observed for the wet catalyst (see Fig. 5b). An increase of predrying/calcination temperature (see Figs. 5c–g) leads to a drastic increase of intensity and to sharpening of the high-temperature sulfiding band around 1000 K. Concomitantly, the sharp low-temperature sulfiding peak

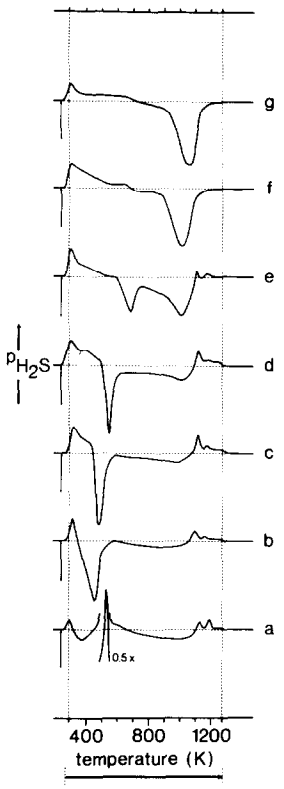

FIG. 5. TPS patterns (10 K/min; H_2S patterns) of Co(3.84)/Al catalysts as a function of calcination temperature and pretreatment. (a) 725 K, wet, addition of 1.0 mol S/mol Co; (b) 725 K, wet; (c) 725 K, dry; (d) 825 K, dry; (e) 925 K, dry; (f) 1025 K, dry; (g) 1175 K, dry. The 50% conversion level of H_2S is indicated by a two-sided arrow.

shifts from 490, via 530, to 680 K when the calcination temperature increases from 725 to 925 K, and decreases in importance with increasing calcination temperature until it is absent for samples calcined at 1025–1175 K. From H_2S and (not shown) H_2 patterns, it is found that interconversion of Co sulfides takes place in the temperature program after calcination at 725–1025 K, while the height of the pattern decreases with increasing calcination temperature. Also the shape of the pattern varies (see Figs. 5a–e). The cooling patterns (not shown) are present in all cases and have the same shape as in Figs. 4a and b, independent of calcination temperature.

Figure 6 gives TPS patterns of dry Co/Al samples as a function of Co content (calcination temperature 725 K). The lower the Co content the harder measurement of TPS patterns becomes. *Wet* catalysts with low Co content, on the one hand, could not be measured because of an extremely large H_2O desorption just above room temperature (see Fig. 4a) which causes a drastic decrease of the stability of the mass signals due to H_2O condensation around the leak valve (*8*). In the case of *predried* catalysts, on the other hand, the H_2O desorption is suppressed sufficiently, but now the H_2S desorption becomes so large that the sulfiding pattern is obscured completely. Consequently, complete TPS of Co(0.20–0.62)/Al could not be measured. In TPS of Co(0.62)/Al, the H_2S desorption problem is avoided by starting the measurement isothermally at 675 K, followed by the temperature program from 675 to 1270 K (see Fig. 6a).

A sharp sulfiding peak around 500 K is only present for the high-loaded Co(2.52–3.84)/Al samples. For all samples a broad high-temperature sulfiding band is found

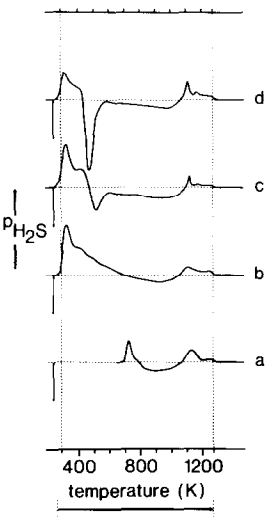

FIG. 6. TPS patterns (10 K/min; H_2S patterns) of Co/Al catalysts calcined at 725 K and predried, as a function of Co content. (a) 0.62 at./nm^2; (b) 1.24 at./nm^2; (c) 2.52 at./nm^2; (d) 3.84 at./nm^2. The TPS measurement on the Co(0.62)/Al sample was started at 675 K instead of at 295 K. The 50% conversion level of H_2S is indicated by a two-sided arrow.

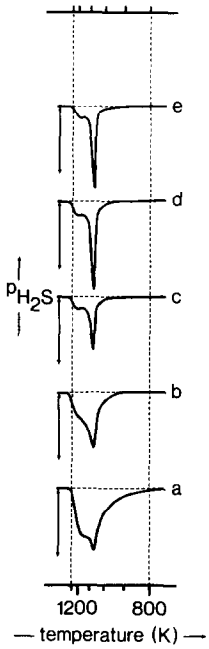

FIG. 7. Cooling patterns after TPS (H_2S patterns; after 30 min isothermally at 1270 K) of Co/Al catalysts calcined at 725 K and predried, as a function of Co content. (a) 0.20 at./nm^2; (b) 0.62 at./nm^2; (c) 1.24 at./nm^2; (d) 2.52 at./nm^2; (e) 3.84 at./nm^2. The 50% conversion level of H_2S is indicated by a two-sided arrow.

which, however, represents only ca. 30% of the total H_2S uptake due to sulfiding, independent of Co content. For the low-loaded Co(0.62–1.24)/Al samples, a H_2S production peak is present around 1100 K, which represents reduction of Al_2O_3 impurities, viz. sulfite and sulfate, as in the case of TPR (see Fig. 2). Interconversion of Co sulfides is observed in all cases. For low Co contents, the interconversion pattern is obscured partly by the reduction of Al_2O_3 impurities. Nevertheless, it can be observed that a broad H_2S production pattern is present independent of Co content, whereas the two distinct peaks are only present for the high-loaded Co(2.52–3.84)/Al samples.

Figure 7 gives the cooling patterns after TPS of dry Co/Al samples as a function of Co content (calcination temperature 725 K). The intensity of the sharp peak at 1070 K clearly decreases with decreasing Co content, whereas a broad band, around 1200 K and tailing to 950–800 K, arises. The latter is not accompanied by a H_2 production band and, therefore, it is concluded that it corresponds with H_2S adsorption on the strongly dehydrated Al_2O_3.

Figure 8 gives the H_2S adsorption in the isothermal stage at 295 K before TPS, as a function of Co content for wet and dry catalysts (calcination temperature 725 K). These values can be calculated from the numbers given in Table 1. The H_2S adsorption is higher for dry than for wet catalysts and also higher for Co/Al samples than for the unloaded support.

DISCUSSION

a. TPS of Crystalline Co Oxides

The TPS patterns of CoO, Co_3O_4, and $CoAl_2O_4$ have led us to the sulfiding scheme shown in Fig. 9. The direct formation of the thermodynamically stable Co sulfides (Reaction 1) seems favorable, via O–S exchange followed by reduction. Some indications, however, are present for intermediate formation of Co metal. First, the large H_2 consumption around 820 K in TPS of CoO (See Fig. 3a) is assigned to reduction of CoO to Co metal (Reaction 2). Second, Co metal has been found by means of XRD after sulfiding of Co_3O_4 at 675 K (*16*). Moreover, the H_2 production peaks around 850–870 K in TPS of CoO and Co_3O_4 (see Figs. 3a–b) point to reaction of

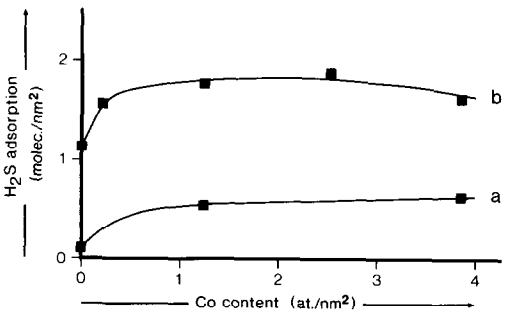

FIG. 8. H_2S adsorption in the isothermal stage at 295 K before TPS on Co/Al catalysts calcined at 725 K, as a function of Co content. (a) Wet catalysts; (b) dry catalysts.

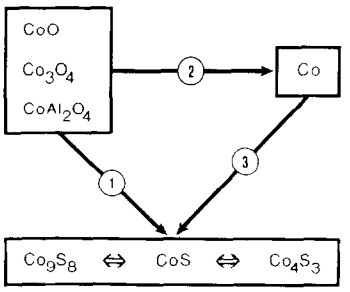

FIG. 9. Sulfiding scheme for crystalline Co compounds. The oxides can be sulfided directly (Reaction 1) or via the intermediate formation of Co metal (Reactions 2 and 3). The Co sulfide formed depends inter alia on the temperature and the H_2S/H_2 pressure ratio applied.

H_2S with a reduced Co species, probably Co metal (Reaction 3), which is in accordance with the easy sulfiding of Co metal at 550–620 K (*17*). Supposedly, Co metal can only be formed in the inner parts of crystallites, which can be reached via micropores where H_2 diffusion is much faster than H_2S diffusion. The same phenomenon has also been observed in sulfiding of MoO_3 (*8*).

The reported nonsulfidability of $CoAl_2O_4$ a 675 K (*5, 18*) agrees well with TPS of $CoAl_2O_4$. With respect to sulfiding of CoO and Co_3O_4, there is more disagreement in the literature; sulfiding has been reported to start around 450 K (*17*), 575 K (*19*), or 675 K (*16*), to be (almost) completed after 2 h at 675 K (*5, 18, 20*), or to continue at low rates in the temperature range 800–1000 K (*21*). In accordance herewith, also the present study shows that different TPS patterns can be obtained after different preparation procedures.

A consistent picture arises for sulfiding of crystallites, when it is supposed that the sulfiding temperature in TPS increases with increasing crystallite size. Such a crystallite size effect has been observed previously in TPS of MoO_2 (*8, 22*). The reaction of H_2S with crystalline oxides starts at the surface, resulting in the formation of a Co sulfide shell which is dense due to the high molar volume of the Co sulfides (*21*). As suggested above, probably some micropores are present allowing H_2 diffusion and some Co metal formation in the bulk, but H_2S diffusion appears to be hindered severely by the shell formation. Consequently, diffusion of Co^{2+} and O^{2-} ions through the Co sulfide product layer might be rate-determining (*17, 21*). The influence of the crystallite size on both ionic diffusion and H_2S gas diffusion explains the following observations:

—Different TPS patterns of CoO and Co_3O_4 after different preparation procedures.

—The easier sulfiding of Co_3O_4 with respect to CoO and the two-peak sulfiding pattern of Co_3O_4 (see Figs. 3a and b). Scanning Electron Microscopy data indicated that, indeed, the CoO particles are much larger than the Co_3O_4 particles (ca. 10 and 1 μm, respectively). Comparison of the latter with the XRD line broadening found for Co_3O_4 suggests that two distinctly differing Co_3O_4 crystallite sizes coexist (ca. 10 nm and 1 μm).

—The much higher sulfiding rate of the well-dispersed Co/Al catalysts in comparison with the crystalline Co oxides (which has been found previously for bulk versus supported Ni and Co oxides (*16, 23*)).

b. Comparison of TPS and TPR Data on Crystalline Co Oxides

TPS patterns alone generally give no unambiguous answer to the question as to whether H_2S or H_2 is the primary reactant during sulfiding (Reactions 1 and 2 in Fig. 9, respectively). Comparison of TPS and TPR results, however, gives additional information on the sulfiding mechanism. The TPR peak maxima (10 K/min) for CoO, Co_3O_4, and $CoAl_2O_4$ lie at 610, 590, and 1150 K, respectively (*7*). Therefore, in TPS of CoO (see Fig. 3a) reduction by H_2 as a first step is not in conflict with the TPR pattern. The higher reduction temperature of CoO in TPS can be explained easily as being caused by blocking by H_2S of the Co metal surface needed for catalytic H_2 dissociation. In the case of Co_3O_4 and $CoAl_2O_4$, sul-

fiding starts far below the temperatures needed for reduction in TPR, excluding H_2 as primary reactant. Apparently, H_2S is the primary reactant via O–S exchange reactions on the low-temperature side of the TPS patterns. It is obvious that reduction by H_2 can become important when the sulfiding temperature reaches the TPR peak temperature. In fact, the crystallite size might determine mainly which is the primary reactant; whereas H_2S supposedly is the primary reactant for small crystallites (low TPS temperatures), the importance of H_2 as primary reactant increases with increasing crystallite size (higher TPS temperatures) due to the more hindered H_2S diffusion into larger crystallites (see Section a).

The very high TPR and TPS peak temperatures found for $CoAl_2O_4$ suggest a different rate-limiting step in this case. It is proposed that solid-state diffusion of Co^{2+} ions is the rate-determining step in both reduction and sulfiding of $CoAl_2O_4$ up to 1000–1100 K. In agreement with this, it has been found that Co^{2+} diffusion starts around 800 K in CoO/Al_2O_3 catalysts (*7*). The slightly lower reactivity in TPR with respect to TPS of $CoAl_2O_4$ can be explained considering that a prerequisite for reduction is the combination of fast Co^{2+} ion diffusion to the surface and fast H_2 dissociation. Therefore, in the case of reduction, on the one hand, an induction period exists in which a minimum amount of Co metal sites (nuclei) is formed which are needed for H_2 dissociation, even when Co^{2+} diffusion is fast. In the case of sulfiding, on the other hand, O–S exchange reactions will occur immediately once the Co^{2+} ions start to diffuse to the surface.

c. TPS of CoO/Al_2O_3 Catalysts

TPS shows that sulfiding of CoO/Al_2O_3 catalysts occurs over an extremely broad temperature range, which is subdivided into a low-temperature sulfiding region (LT; 295–750 K) and a high-temperature sulfiding region (HT; 750–1200 K). The Co species sulfided in the LT and HT region can be considered to be easily sulfidable and hardly sulfidable, respectively, considering the practical sulfiding temperatures of 600–675 K which are maintained for several hours.

In agreement with the importance of sulfiding in the LT region in TPS measurements, the literature shows that significant sulfiding of Co/Al catalysts occurs isothermally at 600–700 K (*3, 5, 16, 24, 25*). While for the high-loaded Co/Al catalysts Co_9S_8 has been observed by XRD (*5, 24, 26, 27*), for the low-loaded Co/Al catalysts also Co sulfide species are formed (*3, 5, 24, 25*), probably CoS species of monolayer type (*5*). Also Mössbauer spectra (*3, 4*) suggest that these Co sulfide species are not identical to Co_9S_8. The formation of Co metal, instead of Co sulfides, has been suggested in an Electron Spin Resonance (ESR) and an X-Ray Photoelectron Spectroscopy (XPS) study (*28, 29*). However, the ESR signal due to Co metal is not reproduced (*26*) and XPS assignments to Co metal are unreliable due to the coincidence of the XPS bands of Co_{2p} electrons of Co metal and Co sulfides (*30*). Moreover, the present study suggests that Co metal can only be formed in sulfiding of large crystallites which do not occur on the Co/Al catalysts. Therefore, it is concluded that Co metal is not a realistic sulfiding product.

Low-temperature sulfiding region (295–750 K). The start of sulfiding at 295 K is evidenced by the observation of color changes. Moreover, from the comparison of H_2S adsorption and desorption data (see Table 1), it follows that part of the adsorbed H_2S does not desorb, i.e., is used for sulfiding reactions in the temperature range 295–500 K. For *wet* catalysts, the amount of physically adsorbed H_2S is small, since only 20–30% of the adsorbed H_2S desorbs in the beginning of the temperature program (295–500 K). It can be observed from Fig. 8 that the H_2S consumption for wet catalysts in this low-temperature sulfiding increases with decreasing Co content, to

ca. 0.5–1.0 mol H_2S/mol Co. The irreversible H_2S adsorption around 675 K by the Co(0.62)/Al sample (see Table 1: A + B = 0.66 mol H_2S/mol Co) indicates that the upper limit for sulfiding up to ca. 675 K lies above this value of 0.66 mol H_2S/mol Co and might be close to 1 mol H_2S/mol Co (i.e., complete sulfiding). The extra adsorption on *dry* catalysts (1.0–1.2 molec. H_2S/nm^2 or 320–380 μmol H_2S/g Al_2O_3) is always compensated by extra desorption and therefore represents physically adsorbed H_2S. This H_2S is associated with the Al_2O_3 surface for the most part, but especially in the low Co concentration range the H_2S adsorption is increased by the presence of Co: there ca. 2 mol H_2S/mol Co are adsorbed besides H_2S adsorption on Al_2O_3 (of which 0.5–1.0 mol H_2S/mol Co is used for sulfiding). The same phenomenon has been found for MoO_3/Al_2O_3 catalysts (*8*). As in the case of low-loaded MoO_3/Al_2O_3 catalysts, the ability to adsorb H_2S might be correlated with the extent of polarization of metal–oxygen bonds: the lower the Co content the more the Co–O bonds are polarized by Al^{3+} ions in the surroundings and the stronger and larger can be the H_2S adsorption. In agreement with this, the TPR results of Fig. 2 show that the reducibility decreases with decreasing Co content, a phenomenon explained previously by polarization (*7*).

The amount of physically adsorbed H_2S on dry catalysts decreases with Co content above ca. 2 at./nm^2, probably due to coverage of Al_2O_3 surface and of Co ions with H_2S adsorption capacity by other Co ions which adsorb less/no H_2S. The same effect might explain the decrease of the NO adsorption on oxidic and sulfided CoO/Al_2O_3 catalysts with increasing Co content (*24, 31*).

Within the LT region also very sharp sulfiding peaks are observed with maxima at 450–680 K for catalysts with high Co contents (2.52–3.84 at./nm^2) calcined at low temperatures (725–925 K). The relatively large H_2 consumption in these peaks indicates that here sulfiding of Co^{3+} ions takes place.

High -temperature sulfiding region (750–1200 K). This region is always observed, but the peak shape and intensity and the temperature range involved vary to a large extent. Catalysts calcined at low temperatures (725–825 K) show broad TPS bands (up to 1100 K) of low intensity, independent of Co content. Much sharper bands of higher intensity are observed at 800–1200 K after calcination at 925–1175 K. In agreement with the increasing importance of the HT region, a decrease of sulfidability with increasing calcination temperature has been reported (*5, 24, 25, 28*). In the HT region the H_2 consumption is always very small indicating that here exclusive sulfiding of Co^{2+} ions takes place.

Due to the high temperatures reached during TPS, one may wonder if a realistic picture of sulfidability of the several Co species is obtained by means of the TPS technique. Especially solid-state diffusion of Co^{2+} ions into the support lattice during TPS might be faster than sulfiding itself, leading to the suggestion of the presence of "nonsulfidable" species (sulfiding in the HT region), whereas these species actually might have been sulfidable in the LT region, if longer reaction times were applied at low temperatures. It has been shown, however, that solid-state diffusion of Co^{2+} ions only takes place above 800 K (*7*). Consequently, the TPS pattern in the LT region (below 750 K) as well as the fraction of the Co species sulfiding in the LT region are not affected by Co^{2+} diffusion. Only the exact position of the TPS peaks within the HT region probably is affected; in this case, Co^{2+} diffusion into the support can retard sulfiding, while Co^{2+} diffusion back to the surface can be the rate-determining step for sulfiding, as is demonstrated for sulfiding of $CoAl_2O_4$ (see Section b).

Interconversion of Co sulfide species. Besides sulfiding at 295–1200 K, complicated patterns due to interconversion of Co sulfide species are found at 1050–1270 K,

which cannot be explained by the normal Co_9S_8–CoS–Co_4S_3 transitions. Apparently, the Al_2O_3 support has a large effect. From the H_2S consumption up to 1270 K (see Table 1) it appears that large fractions of Co_4S_3 are present at 1270 K. In agreement herewith, the cooling patterns after TPS are very similar and, for Co(3.84)/Al samples, the H_2S consumption during cooling comes close to the one required for conversion of Co_4S_3 to Co_9S_8 (see Table 1). However, not all Co is present as Co_4S_3 at 1270 K, since the H_2S consumption during cooling decreases with decreasing Co content (see Table 1). The latter can also be observed in Fig. 7, where the intensity of the sharp peak at 1070 K, assigned to conversion of Co_4S_3 to Co_9S_8, decreases with decreasing Co content. It appears that a significant fraction of the Co (decreasing from 70 to 20% and increasing from 0.15 to 0.8 at./nm^2 with increasing Co content) is strongly interacting with the support, even at 1270 K. Therefore, it is proposed that part of the sulfided monolayer-type surface phase of stoichiometry CoS (5) is strongly stabilized by the support against sintering and predominates especially at the lowest Co contents.

The Co sulfide interconversion patterns can be explained as follows.

—The broad H_2S production "background," which is present up to 1270 K, is tentatively related to reduction of a fraction of the above-mentioned CoS surface phase, after sintering at 1050–1270 K, to Co_4S_3.

—The two H_2S production maxima around 1100 and 1170 K are assigned to reduction of microcrystalline Co sulfides, which were formed by sintering of CoS surface species below 1050 K or by sulfiding of Co oxide crystallites, to Co_4S_3. The observation of different interconversion patterns for bulk oxides and catalysts can be explained by an influence of the crystallite size on the relative thermodynamic stability of the Co sulfides. The fact that the H_2S production and H_2 consumption in Co sulfide interconversion were never larger than 0.12 mol H_2S (mol H_2)/mol Co points to the conversion of microcrystalline Co_9S_8, rather than of CoS, to Co_4S_3. Also the absence of an H_2S consumption peak for the Co_9S_8–CoS transition indicates that crystalline CoS is not formed on the catalysts. The observation of two, instead of one, H_2S production maxima suggests the presence of Co_9S_8 crystallites of two distinctly different sizes, which both reduce in one step to Co_4S_3.

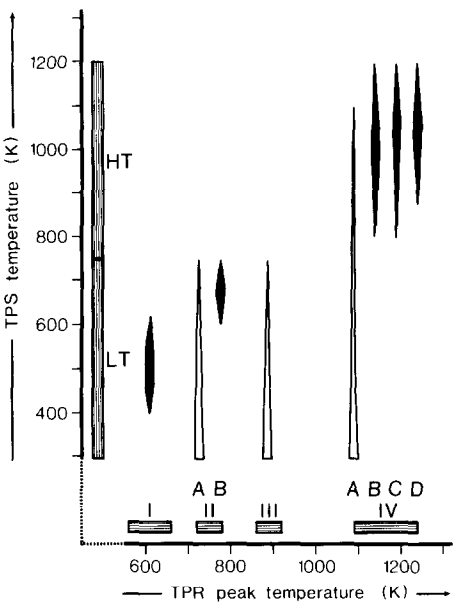

FIG. 10. Correlation of TPR data (horizontal axis) and TPS data (vertical axis) for CoO/Al_2O_3 catalysts. For explanation of the symbols, see Table 2.

d. Comparison of TPS and TPR Data on CoO/Al_2O_3 Catalysts

Since TPR gives detailed structural information on CoO/Al_2O_3 catalysts (7), the correlation of TPS and TPR data on these systems might lead to understanding of the relative sulfidability of the various oxidic Co phases. Table 2 and Fig. 10 give the results of this correlation.

After *calcination at low temperatures* (below 800 K) only Co_3O_4 crystallites (phase I) and various surface phases (IIA,

III, and IVA) can be present (*7*). For catalysts with low Co content (up to ca. 1 at./nm^2), phase IVA predominates (see Figs. 2a–c), whereas sulfiding is already extensive in the LT region, but can only be completed in the HT region (see Figs. 6a and b). Apparently, phase IVA sulfides in both the LT and the HT region. This might be caused by the presence of different Co^{2+} coordinations in phase IVA (*5, 32*): octahedrally and tetrahedrally surrounded Co^{2+} ions are proposed to sulfide in the LT and HT region, respectively. This can be understood considering the need for vacancies in the transition metal coordination where H_2S can adsorb during sulfiding. Sulfiding supposedly is difficult when no vacancies are present nor can it be formed by deformation in the case of the rigid, tetrahedrally surrounded part of phase IVA. However, the octahedrally surrounded part of phase IVA, in spite of its rigidity, is expected to contain more vacancies due to the higher formal coordination number resulting in much higher sulfiding rates.

For catalysts calcined below 800 K, probably *all* sulfiding in the HT region is related to the tetrahedrally surrounded part of phase IVA, whereas the other surface phases (IIA and III besides the octahedrally surrounded part of IVA) as well as Co_3O_4 crystallites (phase I) sulfide in the LT region:

—The surface phases IIA and III have the octahedral surrounding needed for easy sulfiding.
—Small Co_3O_4 crystallites sulfide easily in the LT region (see Section a).
—The fraction of the Co present as phase IVA (ca. 40–100%) is already large enough to explain all sulfiding in the HT region (ca. 30%).

Consequently, the decrease of the Co present as phase IVA from 100 to ca. 40% with increasing Co content is associated with an increase of the fraction of phase IVA which sulfides in the HT region, viz. from 30 to 75%. This can be explained in two ways:

—The fraction of tetrahedral Co^{2+} ions increases as a function of Co content. This is strongly suggested by trends in NO adsorption (*31*) and magnetic susceptibility (*27, 33*) data for Co contents below ca. 1 at./nm^2.
—Part of phase IVA is covered by other Co phases. This has already been mentioned in the above in order to explain the decrease of H_2S adsorption on dry catalysts with increasing Co content (see Fig. 8).

After *calcination at higher temperatures* (above 800 K), diffusion of Co^{2+} ions into the support starts, while above 950 K reduction of Co^{3+} to Co^{2+} in air takes place (*7*). These processes result in the formation of phase IIB at 800–950 K, of phase IVB at 800–1100 K and phase IVC around 1175 K (*7*). Correlation of Figs. 1a–e (TPR) and 5c–g (TPS) shows that an increase of the calcination temperature results in a shift of the sulfiding pattern to the HT region, due to the formation of the hardly sulfidable phases IVB and IVC. Apparently, these phases have the same reduction and sulfiding behavior as the stoichiometric $CoAl_2O_4$ (see Table 2).

Sulfiding of the crystalline phases, I and IIB, supposedly occurs as sharp peaks around 450–680 K, in the LT region:

—The sharpness of these peaks suggests the sulfiding of a homogeneous, probably crystalline phase.
—The H_2 consumption in these peaks points to sulfiding of Co^{3+}-containing phases, such as I and IIB.
—Sulfiding around 400–550 K of Co_3O_4 crystallites (phase I), present after calcination at 725–825 K, is in agreement with TPS of larger, unsupported Co_3O_4 crystallites, taking into account the influence of crystallite size on the TPS sulfiding temperature.
—The increase of the fraction of Co present in the phases I and IIB with increasing Co content correlates with the concomitant increase of the intensity of the sharp sulfiding peaks in the LT region.

—It has been shown that phase I converts into phase IIB when the calcination temperature is increased from 725 to 925 K (*7*). The corresponding increase of the TPR reduction temperatures from 600 to 750 K correlates well with the increase of the TPS sulfiding temperature from 490 to 680 K.

Figure 10 shows that no overall correlation is present between reducibility (measured by TPR) and sulfidability (measured by TPS), since bulk phases behave quite differently from surface phases. For bulk phases alone, however, an excellent correlation exists between TPR and TPS results. For surface phases, such a correlation appears to be absent, but cannot be excluded completely due to the broad TPS signals involved and the interference of H_2S adsorption/desorption phenomena with sulfiding in the LT region.

e. The Sulfiding Mechanism for CoO/Al_2O_3 Catalysts

The sulfiding mechanism is similar to the one found for MoO_3/Al_2O_3 catalysts (*8*):

1. H_2S is the primary reactant in O–S exchange reactions, whereas H_2 plays a secondary role in the reaction mechanism. This can be seen most easily by comparison of TPR and TPS data on the various Co phases (see Table 2 and Fig. 10): reduction takes place at much higher temperatures than sulfiding, especially in the case of surface species. In particular, the high sulfiding rate of octahedrally surrounded Co^{2+} ions of the surface phase IVA is striking in comparison with its extremely low reducibility. This might be explained by the occurrence of concerted cleavage of Co–O bonds and formation of Co–S bonds. The strong Co–O bond, being the main reason for the low reducibility (*7*), is replaced in sulfiding by the even stronger Co–S bond, a process which, if concerted, can be accompanied by a very low activation energy.

2. The (oxy-)sulfides formed by O–S exchange might reduce via cleavage of some Co–S bonds, e.g., surface "Co_2O_3" → surface "Co_2S_3" → 2 surface "CoS", resulting in the formation of elemental sulfur.

3. This sulfur can be easily reduced by H_2 under production of H_2S, catalytically over Co sites up from ca. 400 K (see Fig. 5a) (*34*).

Direct reduction of Co sulfides, i.e., bypassing elemental sulfur as an intermediate, cannot be excluded, since typical H_2S production peaks, observed during TPS of MoO_3/Al_2O_3 (ca. 1 mol H_2S/mol Mo) (*8*), have not been found for CoO/Al_2O_3. However, two good reasons can be given for the lack of H_2S production peaks: (i) the amount of sulfur which can be maximally formed is much smaller in the case of Co catalysts, and (ii) sulfur reduction is catalyzed better by Co than by Mo (*8, 34*) resulting in sulfur reduction as a fast following reaction upon O–S exchange reactions up from ca. 400 K, whereas in the case of Mo catalysts first accumulation of sulfur takes place in the temperature range 295–500 K.

Figures 5b–d indicate that lowering of the H_2O content of the catalysts results in slightly increased sulfiding temperatures, within the LT region. Such an effect of H_2O has been found for MoO_3/Al_2O_3 catalysts and has been explained by catalysis of O–S exchange reactions by Brønsted acid sites occurring especially in the presence of adsorbed H_2O (*8*). Since Brønsted acid sites are not found abundantly on CoO/Al_2O_3 catalysts, another explanation for the influence of H_2O has to be found. A relation might exist with the corrosion of metals, which is more rapid in wet than in dry H_2S. It is suggested that H_2S molecules on the catalyst surface are polarized by the presence of the much more polar H_2O (dielectric constants for H_2O and H_2S (liquid): ca. 78 and 9, respectively). Therefore, (i) the nucleophilicity of H_2S can increase and (ii) the dissociation of H_2S can become easier, resulting in higher sulfiding rates in the presence of H_2O. The explanation given in the case of TPS of MoO_3/Al_2O_3 (Brønsted acidity) corresponds closely with the second explanation given here, since the ease

of H_2S dissociation can be redefined as the extent of Brønsted acidity in the H_2O/H_2S medium.

f. Implications for $CoO–MoO_3/Al_2O_3$ HDS Catalysts

The precursor of the Co phase mainly responsible for HDS activity of sulfided $CoO–MoO_3/Al_2O_3$ catalysts has been reported to be a nonreducible, sulfidable, octahedrally surrounded oxidic Co^{2+} surface species (*2–6, 35, 36*). It is concluded from TPR and TPS measurements that only phase III and the octahedrally surrounded part of phase IVA might be this nonreducible and sulfidable precursor. It is expected that the fraction of these phases and, consequently, the sulfidability are higher for $CoO–MoO_3/Al_2O_3$ than for CoO/Al_2O_3, since it has been reported that the fraction of Co present in octahedral coordination is enhanced by the presence of Mo (*37*). In order to obtain a maximum amount of HDS-active sulfided surface phases, it appears to be necessary to keep the calcination temperature below 800 K, to prevent solid-state diffusion of Co^{2+} ions.

CONCLUSIONS

1. The TPS technique gives a good survey of the relative sulfidability of crystalline Co oxides and of the various Co phases present in CoO/Al_2O_3 catalysts. In the case of catalysts with low Co content, however, the observation of sulfiding in the temperature program is obscured by the extensive sulfiding taking place at 295 K, before TPS, and by H_2S and/or H_2O desorption.

2. Of the crystalline Co oxides, CoO and Co_3O_4 sulfide much more easily than $CoAl_2O_4$. However, especially in the case of CoO and Co_3O_4 a large influence of the crystallite size on the sulfidability is present, which is related to the occurrence of limitations in H_2S gas-phase diffusion and in ionic diffusion through the dense Co sulfide product layer.

3. Sulfiding of Co phases occurs both in a low-temperature (295–750 K) and a high-temperature (750–1200 K) region, representing sulfiding of species which are sulfidable easily and with difficulty, respectively. Octahedrally surrounded surface species as well as supported crystallites sulfide in the LT region. Only a part of the Co^{2+} surface phase IVA, probably tetrahedrally surrounded, as well as subsurface Co^{2+} ions sulfide in the HT region.

4. A positive effect of H_2O on the sulfiding rate is found in the LT region. This is explained tentatively by polarization of H_2S by the much more polar H_2O. This results in more rapid O–S exchange reactions, via increased H_2S nucleophilicity or facilitated H_2S dissociation.

5. Generally, sulfiding in H_2/H_2S (studied by TPS) is much faster than reduction in H_2 (studied by TPR), because of different reaction mechanisms. In sulfiding, H_2S is the primary reactant in O–S exchange reactions, whereas H_2 plays a secondary role, e.g., in reduction of elemental sulfur. H_2 can only compete with H_2S as primary reactant when H_2S diffusion is hindered, i.e., in the case of crystallites.

6. There is no overall correlation between reducibility (measured by TPR) and sulfidability (measured by TPS) of Co phases. Only for crystalline phases is such a correlation found.

7. At 1000–1270 K, interconversion of various crystalline Co sulfides (oxidation/reduction in H_2S/H_2) can be observed. For unsupported crystallites, distinct transitions between Co_9S_8, CoS_{1+x}, and $Co_4S_{3\pm x}$ are observed. For catalysts, the interconversion processes are different, probably due to the presence of small Co_9S_8 crystallites with different thermodynamic stabilities and of a highly stabilized CoS surface phase which sinters slowly and incompletely during TPS, due to strong interaction with the support.

ACKNOWLEDGMENTS

This study was supported by the Netherlands Foundation of Chemical Research (SON) with financial aid from the Netherlands Organization for the Advancement of Pure Research (ZWO). Thanks are due to Dr.

B. Koch and Mr. W. Molleman (Department of X-Ray Spectrometry and Diffractometry, University of Amsterdam) and Mr. C. Bakker (Laboratory for Electron Microscopy, University of Amsterdam).

REFERENCES

1. de Beer, V. H. J., van Sint Fiet, T. H. M., van der Steen, G. H. A. M., Zwaga, A. C., and Schuit, G. C. A., *J. Catal.* **35,** 297 (1974).
2. Wivel, C., Candia, R., Clausen, B. S., Mørup, S., and Topsøe, H., *J. Catal.* **68,** 453 (1981).
3. Topsøe, H., Clausen, B. S., Burriesci, N., Candia, R., and Mørup, S., *in* "Preparation of Catalysts II" (B. Delmon, P. Grange, P. A. Jacobs, and G. Poncelet, Eds.), p. 479. Elsevier, Amsterdam, 1979.
4. Topsøe, H., Clausen, B. S., Candia, R., Wivel, C., and Mørup, S., *J. Catal.* **68,** 433 (1981).
5. Chung, K. S., and Massoth, F. E., *J. Catal.* **64,** 332 (1980).
6. Massoth, F. E., and Chung, K. S., *in* "Proceedings, 7th International Congress on Catalysis, Tokyo, 1980." (T. Seiyama and K. Tanabe, Eds.), p. 629. Elsevier, Amsterdam, 1981.
7. Arnoldy, P., and Moulijn, J. A., *J. Catal.* **93,** 38 (1985).
8. Arnoldy, P., van den Heijkant, J. A. M., de Bok, G. D., and Moulijn, J. A., **92,** 35 (1985).
9. Scheffer, B., de Jonge, J. C. M., Arnoldy, P., and Moulijn, J. A., *Bull. Soc. Chim. Belg.* **93,** 751 (1984).
10. Chung, K. S., and Massoth, F. E., *J. Catal.* **64,** 320 (1980).
11. Moné, R., and Moscou, L., *in* "ACS Symposium Series, No. 20" (J. W. Ward, Ed.), p. 150. Amer. Chem. Soc., Washington, D.C., 1975.
12. Klug, H. P., and Alexander, L. E., "X-Ray Diffraction Procedures," p. 491. Wiley, New York, 1954.
13. Kuznetsov, V. G., Sokolova, M. A., Palkina, K. K., and Popova, Z. V., *Inorg. Mater.* **1,** 617 (1965).
14. Arnoldy, P., van Oers, E. M., Bruinsma, O. S. L., de Beer, V. H. J., and Moulijn, J. A., *J. Catal.* **93,** 231 (1985).
15. Rosenqvist, T., *J. Iron Steel Inst.* **176,** 37 (1954).
16. Erofeev, V. I., Basov, V. G., and Kalechits, I. V., *Kinet. Catal. (Engl. Transl.)* **21,** 393 (1980).
17. Colson, J. C., Delafosse, D., and Barret, P., *Bull. Soc. Chim. Fr.,* 146 (1968).
18. Richardson, J. T., *Ind. Eng. Chem. Fundam.* **3,** 154 (1964).
19. Dumas, P., Steinbrunn, A., and Colson, J. C., *Ned. Tijdschr. Vacuumtech.* **16,** 212 (1978).
20. Medema, J., van Stam, C., de Beer, V. H. J., Konings, A. J. A., and Koningsberger, D. C., *J. Catal.* **53,** 386 (1978).
21. Dumas, P., Colson, J. C., and Fauvre, A., *J. Chem. Res. Miniprint,* 2261 (1977).
22. Arnoldy, P., de Jonge, J. C. M., and Moulijn, J. A., *J. Phys. Chem.,* in press.
23. Dorer, F. H., *J. Catal.* **13,** 65 (1969).
24. Topsøe, N. Y., and Topsøe, H., *J. Catal.* **84,** 386 (1983).
25. de Beer, V. H. J., Bevelander, C., van Sint Fiet, T. H. M., Werter, P. G. A. J., and Amberg, C. H., *J. Catal.* **43,** 68 (1976).
26. Gajardo, P., Grange, P., and Delmon, B., *Surf. Interface Anal.* **3,** 206 (1981).
27. Lo Jacono, M., Cimino, A., and Schuit, G. C. A., *Gazz. Chim. Ital.* **103,** 1281 (1973).
28. Declerck-Grimée, R. I., Canesson, P., Friedman, R. M., and Fripiat, J. J., *J. Phys. Chem.* **82,** 885 (1978).
29. Lo Jacono, M., Verbeek, J. L., and Schuit, G. C. A., *J. Catal.* **29,** 463 (1973).
30. Alstrup, I., Chorkendorff, I., Candia, R., Clausen, B. S., and Topsøe, H., *J. Catal.* **77,** 397 (1982).
31. Topsøe, N. Y., and Topsøe, H., *J. Catal.* **75,** 354 (1982).
32. Grimblot, J., Dufresne, P., Gengembre, L., and Bonnelle, J. P., *Bull. Soc. Chim. Belg.* **90,** 1261 (1981).
33. Tomlinson, J. R., Keeling, R. O., Rymer, G. T., and Bridges, J. M., *in* "Actes du 2me Congr. Int. Catal.," p. 1831. Editions Technip, Paris, 1961.
34. Zazhigalov, V. A., Gerei, S. V., and Rubanik, M. Ya., *Kinet. Catal.* (Engl. Transl.) **16,** 837 (1975).
35. Topsøe, N. Y., and Topsøe, H., *J. Catal.* **77,** 293 (1982).
36. Chiplunker, P., Martinez, N. P., and Mitchell, P. C. H., *Bull. Soc. Chim. Belg.* **90,** 1319 (1981).
37. Ashley, J. H., and Mitchell, P. C. H., *J. Chem. Soc. A,* 2730 (1969).